Environmental Science and Pollution Research (2023) 30:50125–50133
https://doi.org/10.1007/s11356-023-25862-4

RESEARCH ARTICLE

Water level of inland saline wetlands with implications for CO_2 and CH_4 fluxes during the autumn freeze–thaw period in Northeast China

Weijie Wang[1,2] · Hong Liang[1,2] · Feng Li[1,2] · Huihui Su[1,2] · Huiju Li[1,2] · Dawen Gao[1,2]

Received: 10 May 2022 / Accepted: 6 February 2023 / Published online: 15 February 2023

Abstract

Zhalong wetland is the largest inland saline wetland in Asia and susceptible to imbalance and frequent flooding during the freeze–thaw period. Changes in water level and temperature can alter the rate of greenhouse gas release from wetlands and have the potential to alter Earth's carbon budget. However, there are few reports on how water level, temperature, and their interactions affect greenhouse gas flux in inland saline wetland during the freeze–thaw period. This study revealed the characteristics of CO_2 and CH_4 fluxes in Zhalong saline wetlands at different water levels during the autumn freeze–thaw period and clarifies the response of CO_2 and CH_4 fluxes to water levels. The significance analysis of cumulative CO_2 fluxes at different water levels showed that water levels did not have a significant effect on cumulative CO_2 release fluxes from wetlands. Water levels, temperature, soil moisture content, soil nitrate, and ammonium nitrogen content and organic carbon content could explain 24.5–98.9% of CO_2 and CH_4 flux variation. There were significant differences in the average and cumulative CH_4 fluxes at different water levels. The higher the water levels, the higher the CH_4 fluxes. In short, water level had a significant effect on wetland methane fluxes, but not on carbon dioxide fluxes.

Keywords Saline wetland · Autumn freeze–thaw period · Methane · Carbon dioxide

Introduction

Terrestrial ecosystems are major carbon reservoirs and important sources or sinks of greenhouse gases (GHG) (IPCC et al. 2013). Wetlands have higher carbon storage than other ecosystems, accounting for about 20–30% of the earth's soil carbon (Mitsch et al. 2013). Stored carbon is decomposed into CO_2 and CH_4 through soil respiration and methanogenesis (Li et al. 2018). The wetland area in Northeast China is about 1.06×10^4 km^2, accounting for about 16% of total wetland area in China (Di et al. 2004). Activities such as blind reclamation, overgrazing, and construction of artificial reservoirs and ponds have exacerbated the salinization process of wetlands in Northeast China, and more than two-thirds of the wetlands in the Songnen Plain have experienced secondary salinization. As a typical inland alkaline wetland in Northeast China, Zhalong wetland is very sensitive to climate change. In the past 50 years, the annual and seasonal average temperature of Zhalong Wetland has shown an upward trend, and the rainfall has decreased. This has led to an increase in evapotranspiration in the Zhalong Wetland, and the water shortage in the wetland has become increasingly serious. The annual evapotranspiration capacity of Zhalong Wetland is 1506.2 mm (The Ministry of Forestry of the People's Republic of China 1997). Soil alkalization caused by massive evaporation of inland alkaline wetlands is suitable for the growth of methanogenic bacteria and is an important source of methane flux (Liu et al. 2019).

Seasonal freeze–thaw is an important meteorological event in Northeast China, and it impacts the soil ecology and GHG flux characteristics in this area, controls the transfer and transform of the soil nutrient greatly, and affects the chemistry process of mass and energy cycles in the global ecosystems (Liu et al. 2019). Currently, global warming and human activities are changing the structure and function

Responsible Editor: Alexandros Stefanakis

✉ Hong Liang
lianghong@bucea.edu.cn

1 Centre for Urban Environmental Remediation, Beijing University of Civil Engineering and Architecture, Beijing 100044, China

2 Beijing Energy Conservation & Sustainable Urban and Rural Development Provincial and Ministry Co-construction Collaboration Innovation Center, Beijing University of Civil Engineering and Architecture, 100044 Beijing, China

of wetland ecosystems. They can affect GHG fluxes during freeze–thaw periods by water levels, soil properties, and the freeze–thaw process. Water levels are an important determinant of GHG fluxes in a spring-fed forested wetland (Koh et al. 2009). The high water levels in wetlands lead to a hypoxic environment in the soil, which inhibits the autotrophic respiration of plants leading to lower CO_2 fluxes (Koh et al. 2009). The high soil moisture obviously enhanced soil microbial heterotrophic activities and soil microbial respiration in low tidal flats (Hu et al. 2016). In studies of alpine grassland ecosystems on the Tibetan Plateau, the intensity of CO_2 flux reduction decreases as the water levels rises (Zhao et al. 2017). In alpine peatlands, CO_2 fluxes increased significantly with decreasing water levels (Zhang et al. 2020). While CO_2 fluxes were not affected by changes in water levels during a 10-day anaerobic incubation (Toczydlowski et al. 2020), and CH_4 fluxes were mainly limited by water levels, as CH_4 fluxes require an anaerobic environment created by high water levels (Natali 2015). In alpine peatlands, decreasing water levels reduce CH_4 fluxes (Zhang et al. 2020). However, decreasing water levels in chronically flooded wetlands increased CH_4 fluxes (Ding et al. 2002). In general, the effect of water levels on CO_2 and CH_4 fluxes varies according to region differences. Freezing soil can form a better anaerobic environment with unpredictable effects on GHG production (Xiangwen et al. 2019). Spring freeze–thaw cycles inhibit CO_2 fluxes in forests and agroecosystems (Kurganova & Gerenyu 2015). In a German farmland ecosystem, CO_2 fluxes increased during the spring freeze–thaw period instead (Sehy et al. 2004). CH_4 fluxes were also suppressed under spring freeze–thaw cycles in farmland systems of Northern China (Liang et al. 2007), while no significant effect of spring freeze–thaw cycles on CH_4 fluxes in the Zhalong wetland (Liu et al. 2019). The variation of soil properties during the freeze–thaw period could dramatically affect GHG fluxes. The freeze–thaw cycling process during the spring freeze–thaw period leads to a pulsed release of GHG fluxes. Nevertheless, the fluctuation of GHG fluxes and the effect of water levels on GHG sources and sinks have been rarely reported during the autumn freeze–thaw period.

The objectives of this study are to reveal the characteristics of CO_2 and CH_4 fluxes in Zhalong wetlands during the autumn freeze–thaw period and their relationships with water levels. Daily variation of CO_2 and CH_4 fluxes in Zhalong saline wetlands reveals the key environmental drivers causing the differences in GHG fluxes. During the autumn freeze–thaw period, the rainfall in Zhalong wetland decreases, and the water level was lower than that in the growing season. This study contributes to a comprehensive and in-depth understanding of the characteristics of CO_2 and CH_4 fluxes in saline wetlands at different water levels during the autumn freeze–thaw period and clarifies the response of CO_2 and CH_4 fluxes to water levels. This can improve the understanding of GHG sources and sinks in inland saline wetlands and contribute to the construction of regional and even global climate models. The value of the contribution of storage and drainage processes to saline wetland GHG fluxes will be accurately evaluated in the global warming process.

Material and methods

Site description

Zhalong Wetland Nature Reserve (46°52′–47°32′N, 123°47′–124°37′E), a saline wetland, is located in the Songnen Plain, Heilongjiang Province, China. The wetland has a total area of approximately 2100 km^2, 80% of which are reeds (*Phragmites australis*), swampy wetlands. It has a mid-temperate climate, a mean annual air temperature of 3.9 °C, a freezing period of 7 months, and a mean annual precipitation of 420 mm (Gao et al. 2018). The wetland area is low-lying and flat, with numerous marshes distributed. High water levels, poor drainage, and high evaporation lead to soil salinization.

Three water levels points were chosen as study points. The water level above ground at high flooded (HF) point was 7.9–24.8 cm, the main vegetation type is *Phragmites australis* (Table 1). And the water level above ground at middle flooded (MF) point was 1.0–9.5 cm; the main vegetation type is *Phragmites australis* (Table 1). Dry (D) point had no surface water, and the main vegetation types are *Axonopus compressus*, *Medicago Sativa Linn*, and *Imperata cylindrica* (Table 1). The salinities in HF, MF, and D were 87.7 ± 0.08, 101.1 ± 0.12, and 61.8 ± 0.07 mg L^{-1}, respectively (Table 1). The gas was collected from 14 October to 23 November, 2021.

Table 1 The water level and dominant vegetation of the three points

Point	Water level (cm)	Soil salinity (mg L^{-1})	Dominant vegetation
HF	7.9–24.8	87.7 ± 0.08	*Phragmites australis*
MF	1.0–9.5	101.1 ± 0.12	*Phragmites australis*
D	Unflooded	61.8 ± 0.07	*Axonopus compressus*, *Medicago Sativa Linn*, *Imperata cylindrica*

Greenhouse gas flux measurements

The static closed-chamber technique was applied to measure the GHG flux rate (Liu et al. 2019). The chamber consisted of two parts: an open-bottom chamber (50 cm × 50 cm × 50 cm) and a permanent collar (50 cm × 50 cm × 20 cm high). The cubic chambers were made of polypropylene, insulated with expanded polystyrene to minimize temperature changes, and equipped with a battery-driven fan for air circulation through the chambers. During the experimental period, the gutter of the base collar was filled with water to form a water seal. Gas samples were collected every 2 days from 14 October to 6 November, and every 4 days from 11 to 23 November.

Gas sampling was conducted from 9:00 a.m. to 11:00 a.m. (Liu et al. 2019). A full-day sampling started on 23 October, from 7:30 to 19:30 (Xu et al. 2017). A syringe equipped with a three-way screw plug was used to collect 25 mL of gas into a 12-mL vacuum gas bottle at 0, 15, 30, and 45 min (Liu et al. 2019). The concentrations of CH_4 and CO_2 were analyzed by a gas chromatograph (Agilent 7890A) equipped with a methanizer (Ni-catalyst at 350 °C) and a flame ionization detector. The detector temperature was 300 °C, the hydrogen flow was 60 mL min^{-1}, and the air flow was 300 mL min^{-1}. The separation of CH_4 and CO_2 was carried out on a 60/80 mesh 13XMS column with a length of 2 m and an inner diameter of 2 mm. The oven temperature was 55 °C, and the carrier gas was high-purity nitrogen at a flow rate of 20 mL min^{-1}. The soil temperatures at 0 cm, 5 cm, 10 cm, and 15 cm were measured by a portable digital thermometer (JM624, Imin Instruments Ltd., Tianjin, China).

Soil sampling and analysis

Soil samples were collected every 4–5 days from 14 October to 11 November. Soil samples were collected at top (0–10 cm) and bottom (10–20 cm) soil layers, then were screened with a 2-mm sieve. The fresh soil was extracted with 1 mol L^{-1} KCl. NO_3^--N content and NH_4^+-N content were determined using a continuous flow analyzer (SealAnalyticalAA3, Norderstedt, Germany). Soil moisture was measured using the desiccation method. The air-dried soil was used to measure total soil organic carbon, pH, soil salinity, and moisture content (Liu et al. 2019). All experiments were repeated three times.

Statistical analysis

The GHG flux calculation method and data analysis method refer to the previous study (Gao et al. 2019). The data were statistically and analytically analyzed using one-way ANOVA (one-way analysis of variance). It is mainly used to analyze the correlation between the parallel sampling points of each plot and environmental factors and establish a linear model to analyze the significance of the correlation, so as to obtain the interpretation degree of environmental factors to the greenhouse gas emission flux. Fisher's least significant difference method (LSD) was used for multiple comparisons ($\alpha = 0.05$), and the data in the graphs were means ± standard deviations.

Results

Diurnal changes of CO_2 and CH_4 fluxes

The diurnal air temperature varied significantly in the three points. Compared to CH_4, the CO_2 fluxes are more sensitive to temperature, in agreement with the surface air temperature variation (Fig. 1). The air temperature was relatively high at noon, and so did CO_2 fluxes which peaked at 11:30

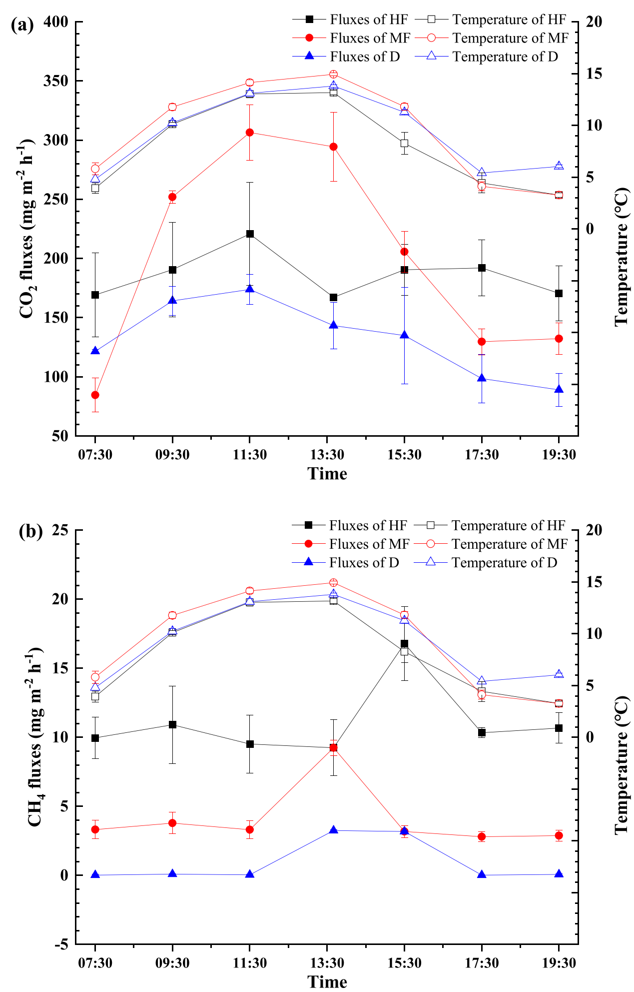

Fig. 1 Diurnal variation of CO_2 and CH_4 fluxes and air temperature from 7:30 to 19:30 during the autumn freeze–thaw period in three types of points. **a** CO_2 fluxes, **b** CH_4 fluxes ($n = 3$)

and were 306.5 (MF), 220.7 (HF), and 173.8 mg m^{-2} h^{-1} (D). The lowest air temperature was 3.3 °C, 3.6 °C, and 1.6 °C at MF, D, and HF, corresponding to CO_2 fluxes (132.3, 98.6, 191.9 mg m^{-2} h^{-1}) and CH_4 fluxes (2.9, 0.0, 10.3 mg m^{-2} h^{-1}).

In HF, the diurnal variation of CO_2 fluxes ranged from 167.3 to 220.7 mg m^{-2} h^{-1}, which maintained a small variation range due to the thermal insulation effect of water. In MF, the CO_2 fluxes ranged from 84.6 to 306.5 mg m^{-2} h^{-1}, which ranged from 89.0 to 173.8 mg m^{-2} h^{-1} in D (Fig. 1a). The CH_4 fluxes changed little with temperature in D (3.3 mg m^{-2} h^{-1}) (Fig. 1b). The peak of CH_4 fluxes of MF and D appeared at the same time (9.2 mg m^{-2} h^{-1}). Due to water insulation, the peak CH_4 fluxes appeared later in HF (16.8 mg m^{-2} h^{-1}).

In MF, CO_2 fluxes were more sensitive to temperature and consistent with surface air temperature changes ($R^2 = 0.962$, $P < 0.01$) (Fig. 2). In D, CO_2 fluxes were significantly positively correlated with 0-cm ($R^2 = 0.695$, $P < 0.01$) and 5-cm ($P < 0.05$) soil temperature (Fig. 2).

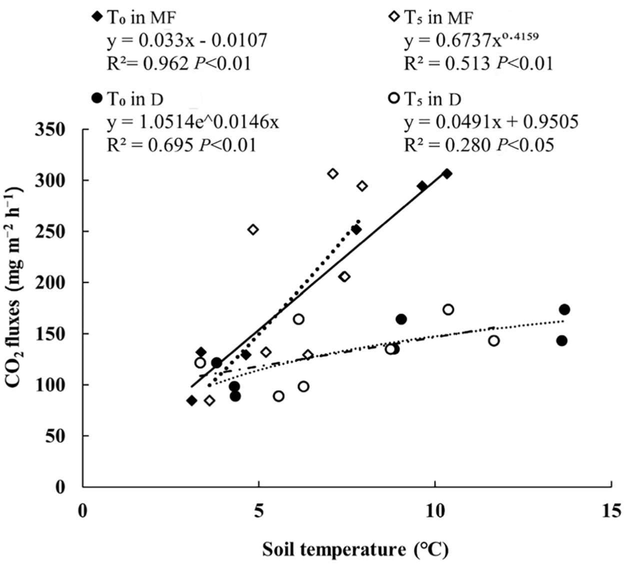

Fig. 2 Model of relationship between the diurnal variation of CO_2 fluxes versus temperature in MF and D. T_0: 0-cm soil temperature, T_5: 5-cm soil temperature

Characteristics of CO_2 and CH_4 fluxes changes

The CO_2 fluxes of the three points all showed a fluctuating downward trend, which represented the source of CO_2 release (Fig. 3a). The range of CO_2 fluxes was 11.3–179.9 mg m^{-2} h^{-1}, 7.6–143.6 mg m^{-2} h^{-1}, and 8.1–164.2 mg m^{-2} h^{-1} in HF, MF, and D, respectively (Fig. 3a). The average and cumulative CO_2 fluxes of HF (83.9 mg m^{-2} h^{-1} and 1594.0 kg hm^{-2}) > D (78.0 mg m^{-2} h^{-1} and 1482.3 kg hm^{-2}) > MF (66.2 mg m^{-2} h^{-1} and 1258.4 kg hm^{-2}) (Fig. 3b).

The ranges of CH_4 fluxes were 3.1–11.9, 2.0–5.4, and 0.0–1.8 mg m^{-2} h^{-1} in HF, MF, and D. The average fluxes are 7.6, 2.5, and 0.3 mg m^{-2} h^{-1} in HF, MF, and D. The trends of CH_4 fluxes were basically the same, showing a

Fig. 3 CO_2 and CH_4 fluxes during the autumn freeze–thaw period. **a** CO_2 fluxes, **b** Cumulative and average CO_2 fluxes, **c** CH_4 fluxes, **d** Cumulative and average CH_4 fluxes

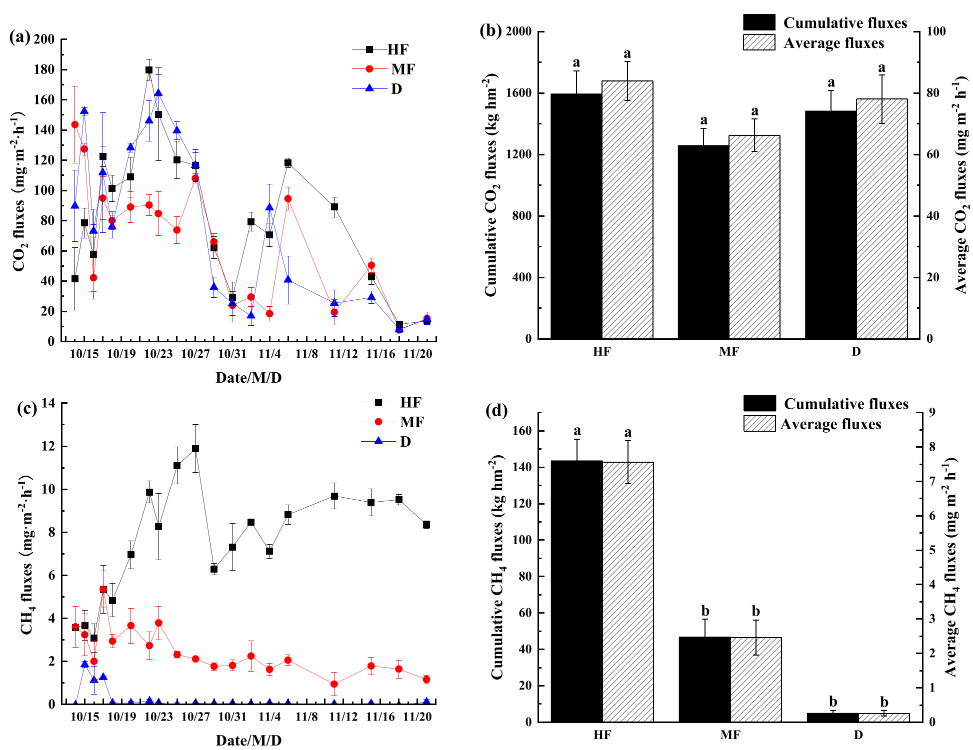

gradual decrease in MF and D (Fig. 3c). While HF showed an increasing trend, first reached a peak and then decreased slightly (Fig. 3c). The CH_4 flux changes coincide with the water levels (Table 3). The average and cumulative CH_4 fluxes of three points varied widely, showing that HF (7.6 mg m^{-2} h^{-1} and 143.6 kg hm^{-2}) > MF (2.5 mg m^{-2} h^{-1} and 46.8 kg hm^{-2}) > D (0.3 mg m^{-2} h^{-1} and 4.9 kg hm^{-2}) (Fig. 3d). It indicates the effect of vegetation on CH_4 fluxes at various water levels.

Correlation of soil CO_2 and CH_4 fluxes with environmental factors

In HF, CO_2 fluxes were only significantly and positively correlated with 0–10 cm soil NH_4^+-N content ($P < 0.05$) (Tables 2 and 3). In MF, CO_2 fluxes were significantly and positively correlated with air temperature ($P < 0.05$) and soil temperature ($P < 0.01$). In D, CO_2 fluxes were significantly positively correlated with air temperature ($P < 0.05$), soil temperature, and 0–10-cm soil moisture content ($P < 0.05$). Soil NH_4^+-N content (0–10 cm) could explain 85.5% of the CO_2 fluxes in HF (Table 4). Air and soil temperature could explain 24.5–61.1% of the CO_2 fluxes in MF and D (Table 4). Soil moisture content (0–10 cm) could explain 98.9% of the CO_2 fluxes in D. In both MF and D, the CO_2 fluxes decreased with the decreasing temperature. In D, the CO_2 fluxes were also influenced by soil moisture content, and the CO_2 fluxes could also increase with the increased moisture content ($P < 0.05$).

In MF, the CH_4 fluxes were significantly and positively correlated with the surface soil temperature ($P < 0.05$) and with 0–10-cm soil NO_3^--N content ($P < 0.05$). In D, the CH_4 fluxes were significantly and positively correlated with 10–20-cm soil moisture content ($P < 0.01$). Zero-centimeter

Table 2 Temperature and other soil physicochemical characteristics of three points

Point type	Soil temperature (℃)				Air temperature (℃)
	0 cm	5 cm	10 cm	15 cm	
D	2.2 ± 0.63a	2.2 ± 0.56b	2.4 ± 0.52b	3.2 ± 0.45b	3.2 ± 1.14a
MF	2.7 ± 0.75b	3.2 ± 0.55b	3.7 ± 0.46b	4.1 ± 0.41ab	3.9 ± 1.17a
HF	5.5 ± 0.97c	4.5 ± 0.70a	4.9 ± 0.50a	4.9 ± 0.47a	4.9 ± 1.08a
Point type	Soil depth (cm)	NO_3^--N (mg kg^{-1})	NH_4^+-N (mg kg^{-1})	pH	TOC (g kg^{-1})
D	0–10	0.2 ± 0.06a	0.1 ± 0.01b	8.5 ± 0.08a	0.1 ± 0.01a
	10–20	0.2 ± 0.06a	0.1 ± 0.03a	8.7 ± 0.12a	0.1 ± 0.01a
MF	0–10	0.2 ± 0.05a	0.1 ± 0.02ab	8. 7 ± 0.03a	0.1 ± 0.01a
	10–20	0.2 ± 0.05a	0.2 ± 0.07a	8.6 ± 0.06a	0.1 ± 0.02a
HF	0–10	0.4 ± 0.15a	0.2 ± 0.04a	8.8 ± 0.18a	0.1 ± 0.01a
	10–20	0.2 ± 0.03a	0.2 ± 0.02a	8.8 ± 0.15a	0.2 ± 0.08a

Significant differences between different samples were tested by multiple comparisons, and different lowercase letters indicate significant differences ($P < 0.05$)

Table 3 Pearson's correlation between GHG fluxes and environmental factors

Related factors	Soil depth (cm)	HF		MF		D	
		CO_2	CH_4	CO_2	CH_4	CO_2	CH_4
Soil temperature	0	0.182	-0.282	0.729 **	0.481*	0.642**	−0.001
	5	0.083	−0.399	0.734**	0.353	0.650**	0.143
	10	0.082	−0.404	0.770**	0.371	0.494*	0.190
	15	0.041	−0.388	0.760**	0.413	0.433	0.275
Air temperature	–	0.321	−0.090	0.553*	0.426	0.494*	−0.088
NO_3^--N content	0–10	0.507	−0.600	0.403	0.912*	0.636	−0.016
	10–20	−0.608	−0.735	−0.441	−0.148	−0.728	0.206
NH_4^+-N content	0–10	0.891*	0.087	−0.404	−0.429	0.505	−0.262
	10–20	0.388	0.849	0.380	−0.394	0.108	−0.420
moisture content	0–10	–	–	0.050	−0.818	0.989*	−0.038
	10–20	–	–	0.404	−0.594	−0.194	0.956*

*Significant effects at $P < 0.05$

**significant effects at $P < 0.01$

Table 4 Correlation of CO_2 fluxes environmental factors

Point	Soil depth (cm)/air	Stepwise multiple linear regression equation	R^2	P value
HF	0–10	$y=185.27\ln(x)+510.02$	0.855	$P<0.01$
MF	0	$y_1=8.9837x_1+42.395$	0.532	$P<0.01$
	5	$y_2=48.423\ln(x_2)+24.528$	0.600	$P<0.01$
	10	$y_3=59.921\ln(x_3)+1.6932$	0.611	$P<0.01$
	15	$y_4=16.835x_4+3.0151$	0.578	$P<0.01$
	Air	$y_5=4.3765x_5+48.848$	0.305	$P<0.05$
D	0	$y_6=8.0709x_6+34.029$	0.412	$P<0.01$
	5	$y_7=20.897e \wedge 0.2227x_7$	0.550	$P<0.01$
	10	$y_8=15.888x_8^{0.9906}$	0.427	$P<0.05$
	Air	$y_9=5.5593x_9+50.6589$	0.245	$P<0.05$

y, y_1, y_2, y_3, y_4, y_5, y_6, y_7, y_8, y_9 was on behalf of CO_2 fluxes; x was on behalf of 0–10 cm soil NH_4^+-N content; x_1, x_2, x_3, x_4, x_6, x_7, x_8 was on behalf of soil temperature; x_5, x_9 was on behalf of air temperature

soil temperature could explain 48.1% of the CH_4 fluxes in the MF. The 10–20-cm soil moisture content could explain 95.6% of the CH_4 fluxes from D. The factors influencing CH_4 fluxes were different in all three points, indicating that CH_4 fluxes were related to point types.

Discussion

Influencing factors of CO_2 and CH_4 diurnal fluxes

The highest CO_2 fluxes of the three points were all at 11:30 a.m., earlier than the highest temperature (13:30 a.m.) (Fig. 1). In the wetlands of northern Jiangsu Province, maximum CO_2 fluxes were also observed slightly earlier than the maximum temperature in October (Xu et al. 2017). The temperature difference from 7:30 a.m. to 19:30 in MF (11.7 °C) was significantly higher than that in HF (9.9 °C) and D (9.0 °C). Accordingly, the fluctuation of CO_2 fluxes was most severe in MF (221.9 mg m^{-2} h^{-1}) than that in HF (53.5 mg m^{-2} h^{-1}) and D (84.9 mg m^{-2} h^{-1}). Due to the multiple influences of plant respiration, plant photosynthesis, soil respiration, and adsorption, the diurnal variation form presented a multimodal pattern (Yuesi et al. 2000).

In this study, the diurnal variation of CH_4 fluxes was generally high in the early afternoon. The largest CH_4 fluxes were also observed in the early afternoon in wetlands in northern Jiangsu Province and the West Siberian peatlands (Veretennikova & Dyukarev 2017, Xu et al. 2017). Anaerobic decomposition of organic matter is the main factor in fluxes of CH_4 (Tsai et al. 2020). Elevated daytime temperatures may promote anaerobic decomposition of organic matter, while lower nighttime temperatures may inhibit the rate of decomposition (Tsai et al. 2020). CH_4 is mainly convective transport with higher transport efficiency during the day, while diffusion transport with lower transport efficiency is the dominant model in the dark (Käki et al. 2001; Van Der Nat et al. 1998). In addition, the CH_4 accumulated at night is released into the atmosphere by convective transport during the day, which also contributes to the high daytime CH_4 fluxes (Turetsky et al. 2014). The three points showed that the CH_4 fluxes increased with the deepening of the water levels, and higher CH_4 fluxes were also observed from fully submerged soils (Turetsky et al. 2014). Moreover, part of the CH_4 is oxidized to CO_2 at night when the water levels are low; the rising CH_4 bubbles also could be oxidized to CO_2 when the water levels are high, so that reducing the CH_4 fluxes (Schrier-Uijl et al. 2011).

Influencing factors of the CO_2 fluxes during the autumn freeze–thaw period

In HF, CO_2 fluxes were significantly positively correlated with 0–10-cm soil NH_4^+-N content ($P<0.05$). The CO_2 fluxes in the remaining two sample points are independent of 0–10 cm soil NH_4^+-N content. Positive correlations between CO_2 fluxes and total CO_2-equivalent fluxes and soil NH_4^+-N content were also observed in mangrove wetlands (Chen et al. 2016). Ammonia nitrogen is conducive to the absorption of nutrients and water by plant roots and promotes soil respiration (Ma et al. 2019). In MF and D, CO_2 fluxes were significantly positively correlated with soil and air temperature (Tables 2 and 3). There was also a significant positive correlation between CO_2 fluxes and soil and air temperatures in the wetlands where reeds were harvested in Zhalong wetland (Liu et al. 2019). The temperature was relatively high in the early stage of the autumn freeze–thaw period. A significant cooling was experienced in early November, resulting in a low point in CO_2 fluxes (18.4 mg m^{-2} h^{-1}, MF; 17.0 mg m^{-2} h^{-1}, D). Then, there was slight warming, and the CO_2 fluxes increased to 94.5 mg m^{-2} h^{-1} (MF) and 88.53 mg m^{-2} h^{-1} (D). Soil temperature enhances soil respiration by accelerating microbial activity and promoting plant root growth, thereby increasing carbon dioxide fluxes (Tang et al. 2020). Moreover, repeated freeze–thaw caused by temperature changes in autumn could increase soil active organic carbon for microbial use (Oztas &Fayetorbay 2003). Soil temperature at 10–15 cm and 0–10 cm had a greater effect on CO_2 fluxes in MF and D, respectively. This suggests that the 10–15-cm and 0–10-cm soil depths are the focal areas for CO_2 production at MF and D, respectively. The CO_2 fluxes at HF are less controlled by temperature. Only in D, CO_2 fluxes were influenced by the 0–10-cm soil moisture content (Tables 2 and 3), which showed a positive correlation. Moisture content impacts soil respiration intensity in agricultural fields and meadows (Cleveland et al. 2010). There was no surface water in D. The oxygen content decreased significantly when the soil moisture content increased; more CO_2 is produced under anaerobic conditions than under aerobic conditions (Walz et al. 2018).

The mean and cumulative CO_2 fluxes were not significantly different in the three points, indicating that water levels and vegetation had no direct effect on CO_2 fluxes, but it can indirectly affect the fluxes of CO_2 by changing soil environmental factors (Fig. 3c). The average CO_2 fluxes is less than the average flux of CO_2 in the northeast permafrost (105.5 mg m^{-2} h^{-1}) (Gao et al. 2022). The reason might be that the temperature drop reduced the respiration activities of microorganisms and plants during the autumn freeze–thaw period, which in turn reduced the CO_2 fluxes. Moreover, the hysteresis between CO_2 fluxes and temperature is higher when the soil moisture content is higher (Gaumont-Guay et al. 2009). Higher water levels delay the effect of temperature on CO_2 fluxes when comparing the CO_2 fluxes in lower water levels.

Influencing factors of the CH_4 fluxes during the autumn freeze–thaw period

In MF, there was a positive correlation between NO_3^--N content of 0–10-cm soil with CH_4 fluxes. The CH_4 fluxes in the remaining two points are independent of NO_3^--N content of 0–10-cm soil. In the anaerobic environment of wetland, there are associated CH_4 oxidizing bacteria that can use nitrate as an electron acceptor to oxidize CH_4, resulting in lower CH_4 fluxes (Ettwig et al. 2016; Shen et al. 2018). The NO_3^--N can promote root growth and root secretion function of marsh plants, and the effective substrate for CH_4-producing bacteria in the roots of marsh plants will increase accordingly (Wang et al. 2012). This promotes the metabolic activity of CH_4-producing bacteria and increases CH_4 fluxes (Wang et al. 2012).

In natural environments, soil moisture content is also an important factor for CH_4 production. Soil moisture can increase the activity of CH_4-producing bacteria and provide anaerobic conditions (Ma et al. 2012). The significant positive correlation between CH_4 fluxes with 10–20-cm soil moisture content only in D. The CH_4 fluxes in the remaining two points are independent of soil moisture content. CH_4 was presented as a flux source in HF, MF, and D with mean values of 7.5, 2.5, and 0.3 mg m^{-2} h^{-1}, respectively. It is much larger than the maximum value of CH_4 flux in northeast paddy fields (0.1 mg m^{-2} h^{-1}) (Zhang et al. 2017). There is a significant positive correlation between water level and CH_4 fluxes. The prolonged overwater condition created an anaerobic environment that is conducive to the growth and reproduction of anaerobic CH_4-producing bacteria, leading to an increase in CH_4 fluxes (Turetsky et al. 2014). The water levels were the key factor affecting the type of methanogens in the soil. In the wetlands of the Qinghai-Tibet Plateau, *Methylobacter* (90.0%) of type I methanotrophs were overwhelmingly dominant in the high water level, while *Methylocystis* (53.3%) and *Methylomonas* (42.2%) belonging to types II and I methanotrophs were the predominant groups in the low water level (Cui et al. 2018). CH_4-producing bacteria are strictly anaerobic, and CH_4-producing bacteria populations are larger in water covered lands (Šťovíček et al. 2017). The higher the water levels and the longer the inundation time, the higher the CH_4 fluxes (Henneberg et al. 2016; Sha et al. 2015). Greater CH_4 fluxes in water-covered wetlands.

Conclusion

Water levels affect the physicochemical properties of wetland soil during the autumn freeze–thaw period. However, water levels could not directly significantly affect the cumulative CO_2 fluxes, but it can indirectly affect the fluxes of CO_2 by changing soil environmental factors. CO_2 fluxes decreased with decreasing air and soil temperatures in MF and D. While CO_2 fluxes were positively correlated with 0–10-cm soil NH_4^+-N content in HF. The water level significantly affects the CH_4 fluxes, the higher the water level, and the higher CH_4 fluxes. Wetlands at lower water levels (below 10-cm water levels) did not show much difference in CH_4 fluxes compared to drylands. CH_4 fluxes increased with decreasing water levels in HF. In MF, CH_4 fluxes were positively correlated with surface temperature and 0–10-cm soil NO_3^--N content. In D, CH_4 fluxes were positively correlated with 10–20-cm soil moisture content. All in all, water level has a significant effect on wetland methane flux, but not on carbon dioxide flux.

Author contribution Weijie Wang: investigation, data analysis, and writing original draft. Hong Liang: supervision, draft revision, funding resources, and conceptualization. Feng Li: data curation, investigation, and writing original draft. Huihui Su: data curation, investigation, and writing original draft. Huiju Li: data curation, investigation. Dawen Gao: conceptualization, supervision and draft revision.

Funding The authors received financial supports by the National Natural Science Foundation of China (No. 31971468).

Data availability All data are mentioned in the body of manuscript, tables, and figure.

Declarations

Ethical approval Not applicable.

Consent to participate Not applicable.

Consent for publication All the authors have read and approved the manuscript and accorded the consent for publication.

Competing interests The authors declare no competing interests.

References

Chen G, Chen B, Yu D, Tam NFY, Ye Y, Chen S (2016) Soil greenhouse gas emissions reduce the contribution of mangrove plants to the atmospheric cooling effect. Environ Res Lett 11:124019. https://doi.org/10.1088/1748-9326/11/12/124019

Cleveland CC, Wieder WR, Townsend R (2010) COS 21–1: experimental drought in a wet tropical forest drives increases in soil carbon dioxide losses to the atmosphere. Ecology 91:2313–2323. https://doi.org/10.2307/27860796

Cui H, Su X, Wei S, Zhu Y, Lu Z, Wang Y et al (2018) Comparative analyses of methanogenic and methanotrophic communities between two different water regimes in controlled wetlands on the Qinghai-Tibetan Plateau. China Curr Microbiol 75(4):484–491. https://doi.org/10.1007/s00284-017-1407-7

Di Z, Y M, W J, H J (2004) Wetlands and their conservation in the Northeast. Geol Res 13: 5

Ding W, Cai Z, Tsuruta H, Li X (2002) Effect of standing water depth on methane emissions from freshwater marshes in Northeast China. Atmos Environ 36:5149–5157. https://doi.org/10.1016/S1352-2310(02)00647-7

Ettwig KF, Zhu B, Speth D, Keltjens JT, Kartal B (2016) Archaea catalyze iron-dependent anaerobic oxidation of methane. Proc Natl Acad Sci 113:12792–12796. https://doi.org/10.1073/pnas.1609534113

Gao D, Liu F, Xie Y, Liang H (2018) Temporal and spatial distribution of ammonia-oxidizing organisms of two types of wetlands in Northeast China. Appl Microbiol Biotechnol 102:7195–7205. https://doi.org/10.1007/s00253-018-9152-9

Gao W, Yao Y, Gao D, Wang H, Song L, Sheng H, Cai T, Liang H (2019) Responses of N_2O emissions to spring thaw period in a typical continuous permafrost region of the Daxing'an Mountains, Northeast China. Atmos Environ 214:1352–2310. https://doi.org/10.1016/j.atmosenv.2019.116822

Gao D, Wang W, Gao W, Zeng Q, Liang H (2022) Greenhouse gas fluxes response to autumn freeze–thaw period in continuous permafrost region of Daxing'an Mountains, Northeast China. Environ Sci Pollut Res 1–15. https://doi.org/10.1007/s11356-022-20371-2

Gaumont-Guay D, Black TA, Mccaughey H, Barr AG, Krishnan P, Jassal RS, Nesic Z (2009) Soil CO_2 efflux in contrasting boreal deciduous and coniferous stands and its contribution to the ecosystem carbon balance. Glob Change Biol 37:1302–1319. https://doi.org/10.1111/j.1365-2486.2008.01830.x

Henneberg A, Brix H, Sorrell BK (2016) The interactive effect of Juncus effusus and water table position on mesocosm methanogenesis and methane emissions. Plant Soil 400:45–54. https://doi.org/10.1007/s11104-015-2707-y

IPCC, Stocker TF, Qin D, Plattner GK, Midgley PM (2013) The physical science basis Contribution of Working Group I to the Fifth Assessment Report of the Intergovernmental Panel on Climate Change. Computational Geometry. https://doi.org/10.1016/S0925-7721(01)00003-7

Käki T, Ojala A, Kankaala P (2001) Diel variation in methane emissions from stands of Phragmites australis (Cav.) Trin. ex Steud. and Typha latifolia L. in a boreal lake. Aquat Bot 71:259–271

Koh HS, Ochs CA, Yu K (2009) Hydrologic gradient and vegetation controls on CH_4 and CO_2 fluxes in a spring-fed forested wetland. Hydrobiologia 630:271–286. https://doi.org/10.1007/s10750-009-9821-x

Kurganova IN, Gerenyu V (2015) Contribution of abiotic factors to CO_2 emission from soils in the freeze–thaw cycles. Eurasian Soil Sci 48:1009–1015. https://doi.org/10.1134/S1064229315090082

Liang W, Shi Y, Zhang H, Yue J, Huang GH (2007) Greenhouse gas emissions from Northeast China rice fields in fallow season. Pedosphere 17:630–638. https://doi.org/10.1016/S1002-0160(07)60075-7

Liu F, Zhang Y, Liang H, Gao D (2019) Long-term harvesting of reeds affects greenhouse gas emissions and microbial functional genes in alkaline wetlands. Water Res 164, 114936.1–114936.10. https://doi.org/10.1016/j.watres.2019.114936

Ma K, Conrad R, Lu Y (2012) Responses of methanogen mcrA genes and their transcripts to an alternate dry/wet cycle of paddy field soil. Appl Environ Microbiol 78:445–454. https://doi.org/10.1128/AEM.06934-11

Ma B, Zhou X, Zhang Q, Qin M, Hu L, Yang K, Xie Z, Ma W, Chen B, Feng H, Liu Y, Du G, Ma X, Le Roux X (2019) How do soil micro-organisms respond to N, P and NP additions? Application of the ecological framework of (co-)limitation by multiple resources. J Ecol 107:2329–2345. https://doi.org/10.1111/1365-2745.13179

Mitsch WJ, Bernal B, Nahlik AM, Mander Ü, Zhang L, Anderson CJ, Jørgensen SE, Brix H (2013) Wetlands, carbon, and climate change. Landscape Ecol 28:583–597. https://doi.org/10.1007/s10980-012-9758-8

Natali SM (2015) Permafrost thaw and soil moisture driving CO_2 and CH_4 release from upland tundra. J Geophys Res Biogeosci 120:525–537. https://doi.org/10.1002/2014JG002872

Oztas T, Fayetorbay F (2003) Effect of freezing and thawing processes on soil aggregate stability. CATENA 52:1–8. https://doi.org/10.1016/S0341-8162(02)00177-7

Schrier-Uijl AP, Veraart AJ, Leffelaar PA, Berendse F, Veenendaal EM (2011) Release of CO_2 and CH_4 from lakes and drainage ditches in temperate wetlands. Biogeochemistry 102:265–279. https://doi.org/10.1007/s10533-010-9440-7

Sehy U, Dyckmans J, Ruser R, Munch JC (2004) Adding dissolved organic carbon to simulate freeze-thaw related N_2O emissions from soil. J Plant Nutr Soil Sci 167:471–478. https://doi.org/10.1002/jpln.200421393

Sha C, Tan J, Wang Q, Wang M (2015) Methane and carbon dioxide emissions from different types of riparian wetland. Ecol Environ Sci 24:1182–1190. https://doi.org/10.16258/j.cnki.1674-5906.2015.07.016

Shen LD, Ouyang L, Zhu Y, Trimmer M (2018) Active pathways of anaerobic methane oxidation across contrasting riverbeds. ISME J 13:752–766. https://doi.org/10.1038/s41396-018-0302-y

Šťovíček A, Kim M, Or D, Gillor O (2017) Microbial community response to hydration-desiccation cycles in desert soil. Sci Rep 7:45735. https://doi.org/10.1038/srep45735

Tang X, Pei X, Lei N, Luo X, Liu L, Shi L, Chen G, Liang J (2020) Global patterns of soil autotrophic respiration and its relation to climate, soil and vegetation characteristics. Geoderma 369:114339. https://doi.org/10.1016/j.geoderma.2020.114339

The Ministry of Forestry of the People's Republic of China (1997) The management programs of Zhalong Nature Reserve. China Forestry Press, Beijing

Toczydlowski A, Slesak RA, Kolka RK, Venterea RT (2020) Temperature and water-level effects on greenhouse gas fluxes from black ash (Fraxinus nigra) wetland soils in the Upper Great Lakes region, USA. Applied Soil Ecology 153:103565. https://doi.org/10.1016/j.apsoil.2020.103565

Tsai C-P, Huang C-M, Yuan C-S, Yang L (2020) Seasonal and diurnal variations of greenhouse gas emissions from a saline mangrove constructed wetland by using an in situ continuous GHG monitoring system. Environ Sci Pollut Res 27:15824–15834. https://doi.org/10.1007/s11356-020-08115-6

Turetsky MR, Kotowska A, Bubier J, Dise NB, Crill P, Hornibrook ER, Minkkinen K, Moore TR, Myers-Smith IH, Nykänen H (2014) A synthesis of methane emissions from 71 northern, temperate, and subtropical wetlands. Glob Change Biol 20:2183–2197. https://doi.org/10.1111/gcb.12580

Van Der Nat F-FW, Van Meteren D, Wielemakers A (1998) Diel methane emission patterns from Scirpus lacustris and Phragmites australis. Biogeochemistry 41:1–22

Veretennikova E, Dyukarev E (2017) Diurnal variations in methane emissions from West Siberia peatlands in summer. Russ Meteorol Hydrol 42:319–326. https://doi.org/10.3103/S1068373917050077

Walz J, Knoblauch C, Tigges R, Opel T, Schirrmeister L, Pfeiffer EM (2018) Greenhouse gas production in degrading ice-rich permafrost deposits in northeastern Siberia. Biogeosciences 15:5423–5436. https://doi.org/10.5194/bg-15-5423-2018

Wang S, Duan J, Xu G, Wang Y, Zhang Z, Rui Y, Luo C, Xu B, Zhu X, Chang X, Cui X, Niu H, Zhao X, Wang W (2012) Effects of warming and grazing on soil N availability, species composition, and ANPP in an alpine meadow. Ecology 93:2365–2376. https://doi.org/10.1890/11-1408.1

Xiangwen S, Ying Z, Dalong J, Hua R, Qiang C, Xingfeng D (2019) Emissions of CO_2, CH_4, and N_2O fluxes from forest soil in Permafrost Region of Daxing'an Mountains, Northeast China. Int J Environ Res Public Health 16:2999. https://doi.org/10.3390/ijerph16162999

Xu X, Fu G, Zou X, Ge C, Zhao Y (2017) Diurnal variations of carbon dioxide, methane, and nitrous oxide fluxes from invasive Spartina alterniflora dominated coastal wetland in northern Jiangsu Province. Acta Oceanol Sin 36:109–117. https://doi.org/10.1007/s13131-017-1015-1

Yu H, Lei W, Xiaohua F, Jianfang Y, Jihua W, Yiufai T, Yiquan L, Ying S (2016) Salinity and nutrient contents of tidal water affects soil respiration and carbon sequestration of high and low tidal flats of Jiuduansha wetlands in different ways. Sci Total Environ 565:637–648. https://doi.org/10.1016/j.scitotenv.2016.05.004

Yuesi W, Baoming J, Yanfen W, Wen Z, Guangren L, Rui D, Dongmei L (2000) Measurement of the exchange rate of greenhouse gases between field and atmosphere in semi arid grassland. Environ Sci 21:6–10. https://doi.org/10.3321/j.issn:0250-3301.2000.03.002

Zhang H, Tang J, Liang S, Li Z, Yang P, Wang J, Wang S (2017) The emissions of carbon dioxide, methane, and nitrous oxide during winter without cultivation in local saline-alkali rice and maize fields in Northeast China. Sustainability 9(10):1916. https://doi.org/10.3390/su9101916

Zhang W, Wang J, Hu Z, Li Y, Yan Z, Zhang X, Wu H, Yan L, Zhang K, Kang X (2020) The primary drivers of greenhouse gas emissions along the water table gradient in the Zoige Alpine Peatland. Water Air Soil Pollut 231:1–12. https://doi.org/10.1007/s11270-020-04605-y

Zhao Z, Dong S, Jiang X, Liu S, Ji H, Li Y, Han Y, Sha W (2017) Effects of warming and nitrogen deposition on CH_4, CO_2 and N_2O emissions in alpine grassland ecosystems of the Qinghai-Tibetan Plateau. Sci Total Environ 592:565–572. https://doi.org/10.1016/j.scitotenv.2017.03.082

Publisher's note Springer Nature remains neutral with regard to jurisdictional claims in published maps and institutional affiliations.